Spontaneous and voltage-activated Ca^{2+} release in adult mouse skeletal muscle fibres expressing the type 3 ryanodine receptor

Claude Legrand[1], Emiliana Giacomello[2], Christine Berthier[1], Bruno Allard[1], Vincenzo Sorrentino[2] and Vincent Jacquemond[1]

[1]*Physiologie Intégrative Cellulaire et Moléculaire, Université Lyon 1, UMR CNRS 5123, Villeurbanne, France*
[2]*Molecular Medicine Section, Department of Neuroscience, University of Siena, Siena, Italy*

The physiological properties and role of the type 3 ryanodine receptor (RyR3), a calcium release channel expressed in a wide variety of cell types, remain mysterious. We forced, *in vivo*, the expression of RyR3 in adult mouse skeletal muscle fibres using a GFP-RyR3 DNA construct. GFP fluorescence was found within spatially restricted regions of muscle fibres where it exhibited a sarcomere-related banded pattern consistent with a localization within or near the junctional sarcoplasmic reticulum membrane. Immunostaining confirmed the presence of RyR3 together with RyR1 within the GFP-positive areas. In ∼90% of RyR3-positive fibres microinjected with the calcium indicator fluo-3, we detected repetitive spontaneous transient elevations of intracellular Ca^{2+} that persisted when fibres were voltage-clamped at −80 mV. These Ca^{2+} transients remained essentially confined to the RyR3 expression region. They ranged from wide local events to propagating Ca^{2+} waves and were in some cases associated with local contractile activity. When voltage-clamp depolarizations were applied while fluo-3 or rhod-2 fluorescence was measured within the RyR3-expressing region, no voltage-evoked 'spark-like' elementary Ca^{2+} release event could be detected. Still global voltage-activated Ca^{2+} release exhibited a prominent early peak within the RyR3-expressing regions. Measurements were also taken from muscles fibres expressing a GFP-RyR1 construct; positive fibres also yielded a local banded pattern of GFP fluorescence but exhibited no spontaneous Ca^{2+} release. Results demonstrate that RyR3 is a very potent source of voltage-independent Ca^{2+} release activity. Conversely we find no evidence that it could contribute to the production of discrete voltage-activated Ca^{2+} release events in differentiated mammalian skeletal muscle.

(Resubmitted 1 October 2007; accepted after revision 9 November 2007; first published online 15 November 2007)
Corresponding author V. Jacquemond: Physiologie Intégrative Cellulaire et Moléculaire, Université Lyon 1, UMR CNRS 5123, Bât. Raphaël Dubois, 43 boulevard du 11 novembre 1918, F69622 Villeurbanne, France.
Email: vincent.jacquemond@univ-lyon1.fr

Ca^{2+} release from the sarco/endoplasmic reticulum through channels belonging to the RyR family is a key signalling mechanism for a wide variety of critical cellular processes. Most well studied is the role of these receptors in the different categories of contractile cells but there is also increasing evidence that RyRs are involved in various aspects of neuronal activity and plasticity as well as in the function of non-excitable cells (for review see Fill & Copello, 2002; Rossi & Sorrentino, 2002; Bruce *et al.* 2003). Of the three identified RyR isoforms, number 1 and number 2 have a clearly identified role in the excitation–contraction (E–C) coupling process of, respectively, skeletal and cardiac muscle and their physiological gating and regulation have been extensively studied and characterized. RyR3, however (Giannini *et al.* 1992), remains poorly known, even though its expression appears somewhat more widespread throughout different tissues than that of RyR1 and RyR2 (Sorrentino, 2003). How and when does RyR3 activity get turned on, how is it regulated, and what is its exact functional role, remain largely open questions.

RyR3 was found expressed in neonatal mammalian skeletal muscle cells together with RyR1 (Tarroni *et al.* 1997; Flucher *et al.* 1999; Conti *et al.* 2005). In accordance with its age-dependent expression, different studies have highlighted the possibility that RyR3 could contribute to E–C coupling during the course

This paper has online supplemental material.

© 2008 The Authors. Journal compilation © 2008 The Physiological Society DOI: 10.1113/jphysiol.2007.145862

of muscle development (Bertocchini *et al.* 1997; Yang *et al.* 2001). Conversely, within most muscles of the adult mammal, essentially only RyR1 remains, being located in the junctional sarcoplasmic reticulum (SR) membrane, where its activity is under the tight control of the voltage-sensing dihydropyridine receptor present in the adjacent transverse tubule membrane. In this configuration RyR1 is directly responsible for the cytoplasmic Ca^{2+} elevation that triggers contraction. Interestingly in certain non-mammalian species, the adult muscle has been shown to contain a roughly equal proportion of two RyR isoforms that are homologous to RyR1 and RyR3 (Lai *et al.* 1992; Oyamada *et al.* 1994; Ottini *et al.* 1996). In these muscles there is also indication that the RyR3 homologue would be located in a para-junctional region of the SR membrane (Felder & Franzini-Armstrong, 2002). This is the case of the adult frog muscle, a benchmark preparation in the E–C coupling field. The question was then raised of whether the presence of RyR3 could be responsible for some of the differences in intracellular Ca^{2+} signalling observed between frog and mammals. A most spectacular one is that membrane depolarization triggers Ca^{2+} sparks in frog muscle whereas it does not in mammalian muscle (Shirokova *et al.* 1998). The possible contribution of RyR3 to Ca^{2+} sparks but also, in a more general manner, to the properties of SR Ca^{2+} release was further investigated using genetically modified cultured myotube preparations expressing either RyR1 or RyR3 or both (Dietze *et al.* 1998; Conklin *et al.* 1999; Shirokova *et al.* 1999; Fessenden *et al.* 2000; Ward *et al.* 2000, 2001). From these studies, and although there is not a complete agreement between the different sets of results, two main lines of conclusions may be drawn: (i) either RyR3 alone or RyR1 alone can produce spontaneous Ca^{2+} sparks with possibly distinct properties; (ii) only RyR1 would be capable of sustaining voltage-activated Ca^{2+} release. Cultured myotubes, however, correspond to a rather immature model of skeletal muscle cells and they exhibit significant differences in terms of electrical properties, ultra-structural organization of membrane compartments and ion channel proteins as compared to the native muscle fibres. So whether the results obtained on this model have physiological relevance in the context of the native tissue remains questionable. Furthermore present data still leave a certain numbers of unsolved issues regarding the role and properties of RyR3. For instance it is still unclear whether or not frog muscle exhibits voltage-activated Ca^{2+} sparks because of the presence of a RyR3 homologue isoform.

In the present work we demonstrate that a functional RyR3 channel can be expressed *in vivo* within adult mouse skeletal muscle fibres. The expression of this channel generates a spontaneous Ca^{2+} release activity that is out of voltage control. Conversely the expressed channel appears incapable of contributing to the production of specific elementary Ca^{2+} release events during physiological E–C coupling. Preliminary aspects of this work were presented to the Biophysical Society (Legrand *et al.* 2007).

Methods

Ethical approval

All experiments and procedures were in accordance with the guidelines of the local animal ethics committee of University Lyon 1, of the French Ministry of Agriculture (87/848) and of the European Community (86/609/EEC).

GFP-RyR1 and GFP-RyR3 plasmids and *in vivo* transfection

RyR1 and RyR3 cDNAs were subcloned into pEGFP-C3 so that the expressed proteins were N-terminally tagged with green fluorescent protein (GFP). The RyR1 cDNA (Nakai *et al.* 1997), kindly provided by Professor P. D. Allen (Department of Anaesthesia, Brigham and Women's Hospital, Boston, MA, USA) was directly subcloned into the *Hin*d III-*Xba* I sites of pEGFP-C3 (Clontech) to obtain GFP-RyR1 plasmid. Subcloning of the RyR3 cDNA from pcDNA3 to pEGFP-C3 was performed in three steps in order to obtain a GFP-RyR3 plasmid.

Swiss OF1 male mice aged 4–6 weeks were used. Transfection was performed within the flexor digitorum brevis (FDB) and interosseus muscles of the animals. Mice were anaesthetized by an intraperitoneal injection of a mixture of ketamine and xylazine dissolved in sterile saline (80 and 16 mg kg^{-1}, respectively). Anaesthesia was checked by loss of the withdrawal reflex induced by toe pinch. Plasmid DNA was then injected into the footpads of the animal using a concentration of 10 μg μl^{-1} in standard Tyrode solution. A 50 μl total volume of this solution was injected in different locations so as to target both the FDB and the interosseus muscles. Following the injection, two flat platinum electrodes were placed on each side of the foot for the electroporation. The standard protocol that we used consisted of 8 pulses of 200 V cm^{-1} amplitude and 20 ms duration delivered at a frequency of 2 Hz by a BTX ECM 830 square wave pulse generator (Harvard Apparatus, Holliston, MA, USA). Experimental observations and measurements were carried out 2 weeks later. This 2 week delay was chosen on the basis of early tests done with expression of the RyR3-GFP construct but also of GFP alone and of another GFP-tagged ion channel protein unrelated to the present project. For these three plasmids, using the same conditions of transfection as in the present work, a delay of approximately 10–14 days was found to provide the largest number of positive fibres in a reproducible manner. Positive fibres could be found at earlier (from 5 days post transfection) and also later

© 2008 The Authors. Journal compilation © 2008 The Physiological Society

times (up to 3 weeks) but in lower density and more unpredictable manner.

Fluorescent immunolabelling and confocal microscopy

Frozen sections were prepared from the transfected muscles, frozen in liquid nitrogen and longitudinally sectioned with a Leica cryostat. Sections (8 μm) were fixed with 3% paraformaldeyde in PBS for 7 min at room temperature and then extensively washed with PBS plus 0.2% BSA. Sections were blocked for 2 h at 25°C in PBS containing 0.2% BSA and 5% goat serum and then incubated overnight with primary antibodies. Sections were washed three times with PBS–0.2% BSA and incubated for 20 min with PBS–2% BSA; a Cy3-conjugated secondary antibody (Jackson Immunoresearch) was then applied for 1 h at 25°C. Sections were washed three times, mounted with a Mowiol mounting medium (Calbiochem) containing 0.025% DABCO and analysed with a Zeiss LSM510 Meta confocal microscope.

Preparation of the isolated muscle fibres

Single fibres were isolated from the FDB and interosseus muscles from mouse using a previously described procedure (Jacquemond, 1997). In brief, mice were killed by cervical dislocation before removal of the muscles. Muscles were treated with collagenase (Sigma, type 1) for 60 min at 37°C. Single fibres were then obtained by triturating the muscles within the experimental chamber. For standard observations performed in the absence of voltage clamp, fibres were bathed either in Tyrode solution or in culture medium with 10% FBS (M199, Eurobio, France). Fibres were observed either with a conventional inverted microscope (Olympus IMT2 or Nikon Diaphot) equipped for epifluorescence with a fluorescein-type filter set or with the laser scanning confocal microscope available at the Centre Technologique des Microstructures of University Lyon 1 (see below). Fibres were dispersed on the bottom of either a standard 35 mm Petri dish or, for the confocal measurements, of a single-well Lab-Tek chamber (Nalge Nunc, Naperville, IL, USA).

For intracellular Ca^{2+} measurements fibres were first partially insulated with silicone grease as previously described (Jacquemond, 1997); in brief fibres were embedded within silicone so that only a portion of the fibre extremity was left out of the silicone, in contact with the bathing medium. Under these conditions fibres remained well maintained on the bottom of the chamber and this also allowed whole-cell voltage clamp to be achieved on the silicone-free extremity of the fibre, when needed. Transfected fibres were handled with silicone so that the fibre region exhibiting GFP fluorescence was left out of the silicone. It should be noted that all GFP-positive fibres were not eligible for this procedure, especially when the region of expression was within the central portion of the fibre. Once partially embedded within silicone, fluo-3 (or rhod-2) was introduced into the myoplasm through local pressure microinjection with a micropipette containing 1 mM of the dye dissolved in an intracellular-like solution (see Solutions). Microinjection was always performed within the silicone-embedded part of the fibre, away from the silicone-free end portion under study. Following diffusion and equilibration within the cytoplasm, this was believed to achieve a final cytoplasmic concentration within the 100–200 μm range (for details concerning microinjections see Csernoch *et al.* 1998).

For measurements performed on frog fibres (Fig. 6*D*), animals were killed by decapitation and pithed. Single fibres were enzymatically isolated from the toe muscles using the same procedures and solutions as for the mouse muscles. Voltage clamp and fluo-3 fluorescence measurements were also achieved using identical conditions to those used for the mouse fibres. All experiments were performed at room temperature (20–22°C).

Confocal fluorescence measurements on isolated fibres

Fibres were visualized using the Zeiss LSM 510 laser scanning confocal microscope available at the Centre Technologique des Microstructures of University Lyon 1. The microscope was equipped with a × 63 oil immersion objective (numerical aperture 1.4).

For detection of both GFP and fluo-3 fluorescence the excitation was provided by the 488 nm line of an argon laser and a 505 nm long pass filter was used on the detection channel. For the series of measurements performed with rhod-2 (experiments relating to Fig. 8) the excitation was from the 543 nm line of a HeNe laser and fluorescence was collected above 560 nm. Intracellular $[Ca^{2+}]$-related fluorescence changes were either imaged by repetitive scanning of a given confocal field or by using the line-scan mode of the system. Image processing and analysis was performed using Image/J (NIH, USA) and Microcal Origin (Microcal Software Inc., Northampton, MA, USA). As described in Results the expression of the RyR constructs was not homogeneous throughout the transfected fibres; as a consequence once a fibre had been injected with the dye fluo-3, the fluorescence of the dye made the precise identification of the exogenous RyR expression area more complicated. This was particularly important when investigating the properties of voltage-activated Ca^{2+} release events in RyR3-expressing regions (results described in relation to Fig. 6). In order to ensure that these measurements were indeed taken from that area we relied, in most cases, on an image of the GFP-RyR fluorescence taken before fluo-3 was injected. Furthermore, in most

© 2008 The Authors. Journal compilation © 2008 The Physiological Society

cases the GFP-RyR expression area could still easily be inferred (despite the presence of fluo-3) by the presence of a high intensity zone of fluorescence in the vicinity of a nucleus present in that expression region. Finally and as described in Results, the RyR3-expressing area exhibited spontaneous Ca^{2+} transients; the presence of spontaneous activity within the scanned area was thus taken as an index of the presence of RyR3 within that region.

Changes in fluorescence were expressed as $\Delta F/F$ where F is the resting (or baseline) fluorescence level. When fluo-3 fluorescence was measured from an area of fibre expressing a GFP-RyR construct, one obvious difficulty was that the absolute $\Delta F/F$ value due to a given change in $[Ca^{2+}]$ was underestimated because of the contribution of GFP to the baseline fluorescence. This was also complicated by the fact that the GFP fluorescence intensity was not homogeneous within the expression area. For this reason, a rigorous quantitative comparison of the Ca^{2+}-related $\Delta F/F$ fluo-3 signals between GFP-RyR-expressing areas and control areas was precluded. In an attempt to estimate the corresponding error, we took, in four fibres, images from the same field exhibiting GFP fluorescence, before and after fluo-3 had diffused and equilibrated throughout the myoplasm. Comparison of the two images indicated that within the strongest expression area, the final fluorescence level corresponded approximately to 2–3 times the initial GFP level. Under these conditions any $\Delta F/F$ signal from this area would be underestimated by ∼30–50%.

Conversely, GFP did not interfere with rhod-2 fluorescence. A specific series of measurements was thus performed with this dye in order to rigorously compare the global Ca^{2+}-related $\Delta F/F$ signals elicited by voltage-clamp depolarization in GFP-RyR3-expressing areas and control areas of muscle fibres. Changes in $[Ca^{2+}]$ were calculated from the rhod-2 signals using the previously described pseudo-ratio equation (Cheng *et al.* 1993) assuming a basal $[Ca^{2+}]$ of 100 nM and a K_d of rhod-2 for Ca^{2+} of 0.6 μM. An estimation of the Ca^{2+} release flux underlying the thus calculated global $[Ca^{2+}]$ transients was performed according to previously described procedures (Collet *et al.* 2004; Pouvreau *et al.* 2006). In brief, the SR calcium release flux was calculated from the time derivative of the total myoplasmic Ca^{2+} obtained from the occupancy of intracellular calcium binding sites. The model included troponin C-binding sites with a total sites concentration TN_{total} of 250 μM, an 'on' rate constant $k_{on,CaTN}$ of 0.0575 μM^{-1} ms^{-1} and an 'off' rate constant $k_{off,CaTN}$ of 0.115 ms^{-1}; Ca^{2+}–Mg^{2+} binding sites on parvalbumin with a total sites concentration $PV_{total} = 2000$ μM, 'on' rate constant for Ca^{2+} $k_{on,CaPV} = 0.125$ μM^{-1} ms^{-1}, 'off' rate constant for Ca^{2+} $k_{off,CaPV} = 5 \times 10^{-4}$ ms^{-1}, 'on' rate constant for Mg^{2+} $k_{on,MgPV} = 3.3 \times 10^{-5}$ μM^{-1} ms^{-1}, 'off' rate constant for Mg^{2+} $k_{off,MgPV} = 3 \times 10^{-3}$ ms^{-1}. Calcium transport across the SR membrane was included with a rate assumed to be proportional to the fractional occupancy of the SR pump sites with a Ca^{2+} pump K_d of 2 μM and a maximum pump rate of 10 μM ms^{-1}. Resting $[Mg^{2+}]$ was assumed to be 1.5 mM.

Electrophysiology

An RK-400 patch-clamp amplifier (Bio-Logic, Claix, France) was used in whole-cell configuration. Fibres were bathed in the TEA-containing extracellular solution (see Solutions). Command voltage pulse generation was achieved with an SMP300 voltage pulse generator (Bio-Logic). Analog compensation was systematically used to decrease the effective series resistance. Voltage clamp was performed with a microelectrode filled with the intracellular-like solution (see Solutions). The tip of the microelectrode was inserted through the silicone, within the insulated part of the fibre. Membrane depolarizations were applied from a holding command potential of −80 mV.

Solutions

The intracellular-like solution contained (mM) 120 potassium glutamate, 5 Na_2-ATP, 5 sodium phosphocreatine, 5.5 $MgCl_2$, 5 glucose, 5 Hepes adjusted to pH 7.20 with KOH. The extracellular solution used for whole-cell voltage clamp contained (mM) 140 TEA-methanesulphonate, 2.5 $CaCl_2$, 2 $MgCl_2$, 10 TEA-Hepes and 0.002 tetrodotoxin, pH 7.20.

Results

RyR3 expression

GFP fluorescence was detected in a very small proportion of the total number of fibres isolated from the transfected muscles. Following collagenase treatment a transfected muscle commonly revealed ∼20–30 healthy-looking fibres exhibiting GFP fluorescence. The maximum number of GFP-positive fibres that we could obtain was ∼90 from one interosseus muscle. Although small, the number of positive fibres obtained under our standard conditions was sufficient to allow a functional characterization of the consequences of RyR3 expression in this model. Figure 1*A–D* presents four sets of a given transmitted light image (left) and of the corresponding confocal fluorescence image (right), taken from muscle fibres expressing the GFP-RyR3 construct. One hallmark of the expression profile was that it was always local and usually distributed around one nucleus as clearly exemplified in Fig. 1*A*. The apparent surface area of fibres where fluorescence was detected typically ranged between 1000 and 3000 μm^2. In some cases fibres exhibited two spots of RyR3 expression (Fig. 1*C*) and infrequently three or more (Fig. 1*D*). Another typical feature of the expression profile

© 2008 The Authors. Journal compilation © 2008 The Physiological Society

was that it showed a striated pattern running perpendicular to the longitudinal axis of the fibre, consistent with a sarcomere-related localization of the protein. This is shown more closely in Fig. 1*E*–*H*. Figure 1*E* shows the transmitted light image taken from a RyR3-positive fibre and Fig. 1*F* shows a corresponding confocal image of the GFP fluorescence. Figure 1*G* and *H* shows the average intensity profile from the white box region in the above corresponding images. The intensity profile in the transmitted light image showed the classic repeats of peaks and

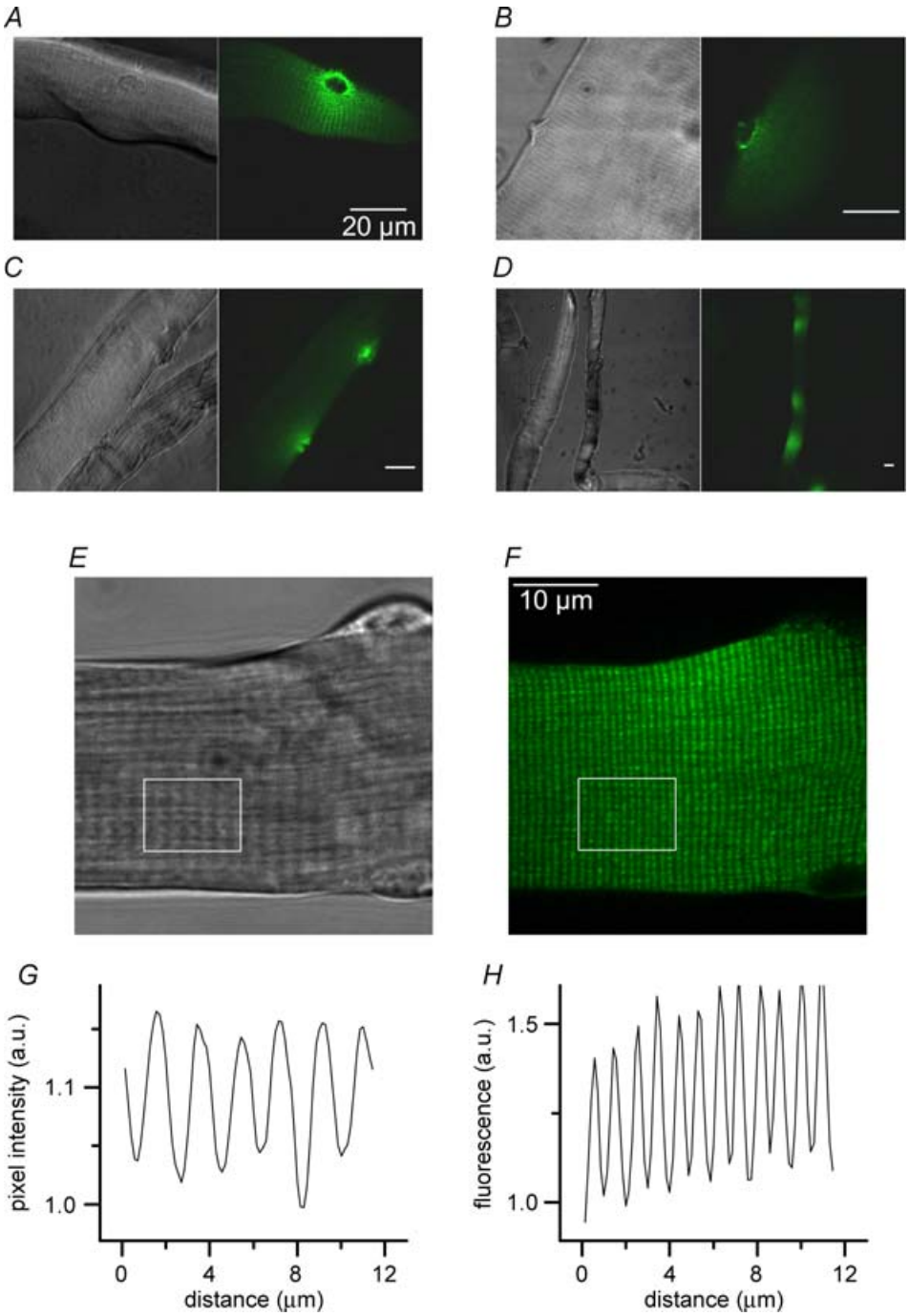

Figure 1. Pattern of RyR3 expression in transfected mouse skeletal muscle fibres
A–D, pairs of images including a confocal fluorescence frame (right) and the corresponding transmitted light image (left) taken from muscle fibres expressing the GFP-RyR3 construct. *E* and *F*, higher magnification transmitted light image and corresponding confocal image of the GFP fluorescence from a RyR3-positive end of fibre, respectively. *G* and *H*, average intensity profile from the white box region in the above corresponding images.

© 2008 The Authors. Journal compilation © 2008 The Physiological Society

valleys corresponding to the *A* and *I* bands, respectively, indicative of a sarcomere length of approximately 2 μm. The intensity profile in the fluorescence image also showed a banded pattern but with a higher frequency. From measurements taken in 12 RyR3-positive fibres the mean spacing between adjacent peaks of fluorescence was 1.0 ± 0.04 μm. Since it is known that in mammalian muscle there are two t-tubules per sarcomere, the present pattern of GFP fluorescence is consistent with RyR3 being localized within the t-tubule-junctional SR region.

Immunolocalization of GFP-RyR3 fusion protein in FDB-transfected fibres

In order to verify the subcellular localization of the GFP-RyR3 fusion protein, muscle cryosections from tranfected FDB muscles were stained with a monoclonal antibody against α-actinin, a monoclonal antibody (34C) which recognizes all RyR isoforms, or using either a RyR1- or a RyR3-specific rabbit antibody. As shown in Fig. 2, the GFP-RyR3 fluorescence was observed as a double band located on both sides of the signal obtained with a monoclonal antibody against α-actinin, which labels the Z-disk region of the sarcomere. This data indicated that the GFP-RyR3 protein was localized in correspondence to the A–I junctions, where triads are located. The triadic signal at the level of the A–I junctions was the only signal observed using the 34C antibody which recognizes all RyR isoforms. The triadic localization of the GFP-RyR3 was further confirmed by its colocalization with the staining of the endogenous RyR1. Finally, the identity of the GFP fusion protein was verified by staining with a RyR3-specific antibody.

Spontaneous Ca^{2+} release activity in the RyR3-expressing fibres

Figure 3*A* shows a confocal image of the GFP fluorescence from a RyR3-positive fibre. The image was taken immediately after fluo-3 had been injected within the fibre end that was the most distant from the GFP-positive region (see Methods). Figure 3*B* was taken 20 min later, while fluo-3 was equilibrating throughout the entire myoplasmic volume. Figure 3*C* presents a series of consecutive confocal frames taken from that same area at a frequency of 1.25 Hz. There were clear transient changes in fluo-3 fluorescence originating from the RyR3-expressing region (see also online Supplemental material, movie 1). In this example, the transient $[Ca^{2+}]$ elevations appeared to initially spread over either one or the other side of the region where the RyR3 expression seemed the highest and later on a more extended semicircular area. Figure 3*D* shows the time

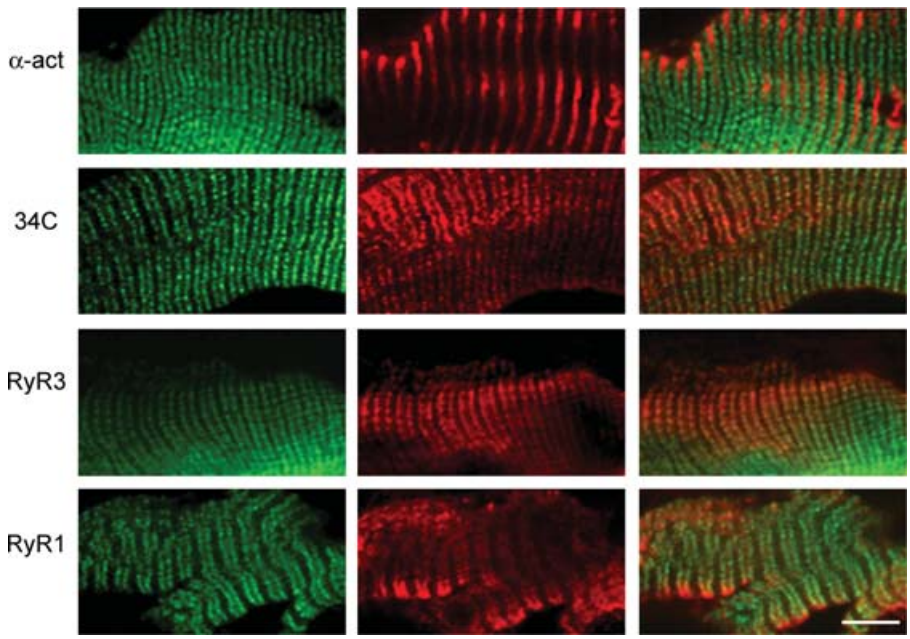

Figure 2. Immunofluorescence labelling of RyR3-expressing muscle fibres
Representative labelling patterns of GFP-tagged RyR3-expressing fibres after immunolabelling of muscle cryosections with (from top to bottom) a monoclonal mouse antibody against α-actinin, a mouse monoclonal antibody recognizing all RyR isoforms (34C), a polyclonal rabbit antibody raised against RyR3, and a polyclonal rabbit antibody raised against RyR1. The left column shows the GFP-RyR3 fluorescence. The middle column shows the corresponding immunolabelling. The right column shows the two merged images. The scale bar indicates 10 μm.

© 2008 The Authors. Journal compilation © 2008 The Physiological Society

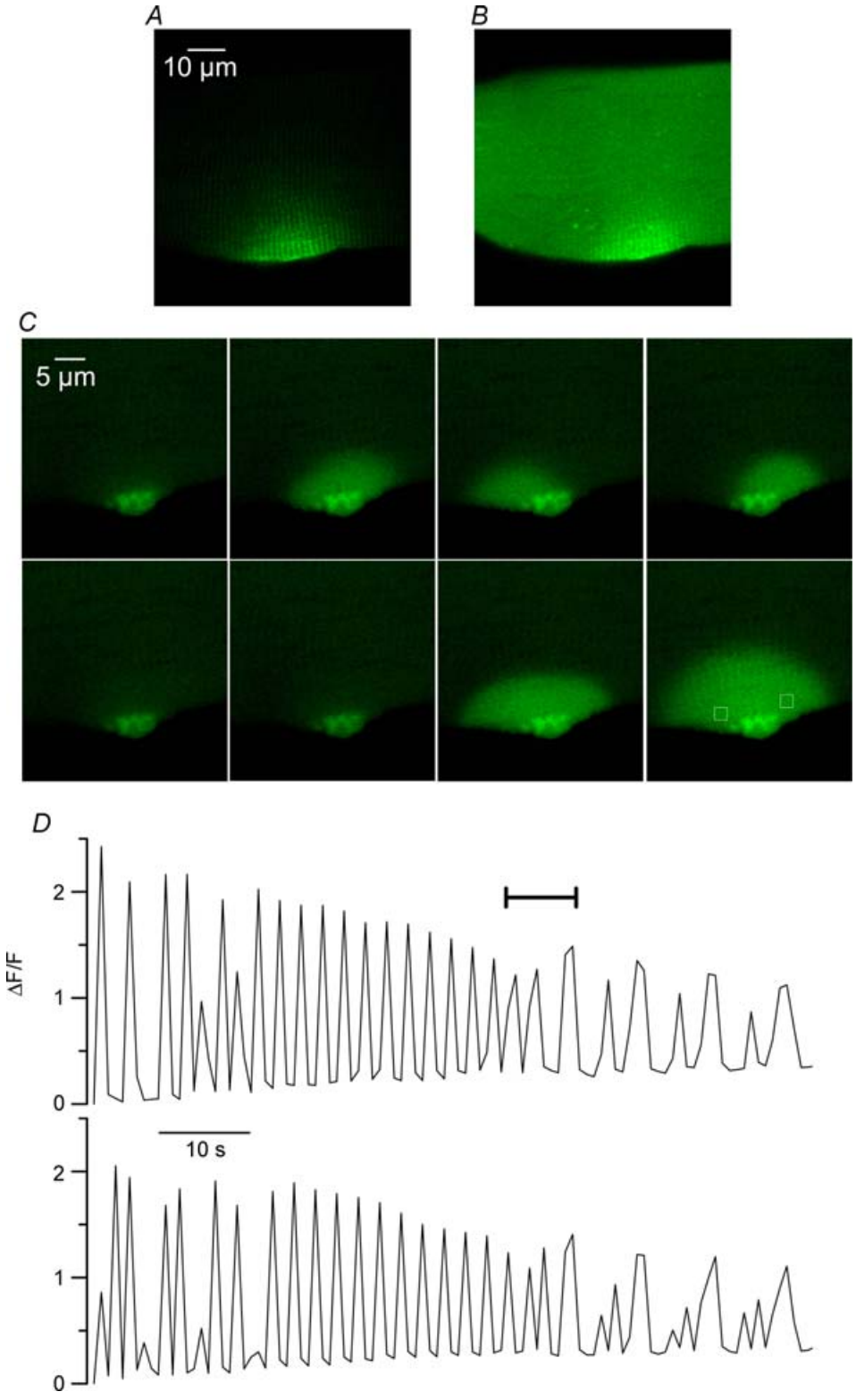

Figure 3. Spontaneous cytoplasmic [Ca^{2+}] oscillations in RyR3-expressing muscle fibres
A and *B*, confocal fluorescence images taken from a RyR3-expressing region of fibre before (*A*) and 20 min after fluo-3 had been injected (*B*). *C*, series of consecutive confocal frames taken at a frequency of 1.25 Hz from the area shown in *A* and *B*. *D*, time course of the normalized change in fluorescence measured from the two regions highlighted by white boxes in the last image of *C* (top trace corresponds to the left box); the period of time corresponding to the images shown in *C* is indicated by a horizontal bar.

© 2008 The Authors. Journal compilation © 2008 The Physiological Society

course of the normalized change in fluorescence measured from the two regions highlighted by a white box in the last image of Fig. 3*C* (top trace corresponds to the left box). The period of time corresponding to the images shown in Fig. 3*C* is indicated by a horizontal bar. Although the time resolution was poor, traces indicate that these spontaneous transients, that we also refer to as $[Ca^{2+}]$ oscillations, occurred at a frequency of ∼0.5–0.2 Hz and reached a peak $\Delta F/F$ value of ∼2. The traces also stress the fact that over the first 50 s of the record, $[Ca^{2+}]$ rose alternately within and around one of the two regions of interest. Thereafter $[Ca^{2+}]$ was transiently increasing in a synchronous manner within the two regions while both the frequency and amplitude of the oscillations tended to decrease. Although variable in spatial pattern, amplitude and frequency, such spontaneous Ca^{2+} oscillations were detected in 24 out of 27 RyR3-positive fibres that were injected with fluo-3. They occurred at a frequency that ranged between 0.06 and 0.15 Hz, and usually reached peak $\Delta F/F$ values of ∼1–2. They appeared to always remain confined within the RyR3-expressing region of fibre and were never observed in control fibres. They could be detected in RyR3-positive fibres voltage-clamped at −80 mV ($n = 5$) which rules out the possibility that they would be induced by changes in membrane polarization. Furthermore they could also be detected in fibres that were bathed in the absence of extracellular calcium ($n = 2$), excluding the possibility that they would result from Ca^{2+} entry from the external medium (Fig. 5*B*). Overall there is thus no doubt that these Ca^{2+} oscillations resulted from local spontaneous SR Ca^{2+} release.

The properties of these spontaneous Ca^{2+} release signals were further examined using the line-scan mode of the confocal system. Results shown in Fig. 4 were obtained from a RyR3-positive fibre that had been injected with fluo-3 and voltage-clamped at −80 mV with the silicone voltage-clamp technique (see Methods). The silicone-free end of the fibre is clearly seen in the transmitted light image shown in Fig. 4*A*. The region where RyR3 was expressed was located within that silicone-free portion of fibre, still witnessed (despite the presence of fluo-3) by a high intensity spot of fluorescence on the top part of the fibre (Fig. 4*B*). Figure 4*C* shows an enlarged confocal view of the RyR3-positive area; the horizontal line corresponds to the position of a single line that was scanned every 13.8 ms. The (x,t) image in Fig. 4*D* was obtained from a portion of that line where repetitive Ca^{2+} release events were detected. Events occurred at a frequency of ∼0.2 Hz and spread spatially over a total distance of ∼20 μm. The time course of relative change in fluorescence at two distinct locations of the line is shown above and below the image. There were at least two active spots that operated either synchronously or with a slight delay. This is also illustrated in Fig. 4*E* which shows an enlarged view of the two first events in Fig. 4*D*. From measurements of such local spontaneous events detected in line-scan mode in five RyR3-positive fibres, mean values for peak amplitude, width at half-peak amplitude and full duration were 1.1 ± 0.4 $\Delta F/F$, 14.7 ± 3 μm and 1.7 ± 0.3 s, respectively. Although these events exhibited qualitative features similar to those of the conventional spontaneous Ca^{2+} sparks observed in frog muscle, both the duration and the spacewidth were at least one order of magnitude larger (see for instance Table 2 from Baylor, 2005).

As already mentioned, the spatio-temporal properties of the spontaneous Ca^{2+} oscillations were variable from fibre to fibre. For instance, in some cases RyR3 expression generated travelling or propagating Ca^{2+} waves as exemplified in Fig. 5*A*. In some fibres the spontaneous Ca^{2+} release activity was responsible for local contractions (see Supplemental movie 2).

Voltage-induced fluo-3 Ca^{2+} signals in RyR3-expressing fibres

RyR3 has been suspected of being responsible for the presence of voltage-activated Ca^{2+} sparks in frog muscle. It was thus of specific interest to test the occurrence of such events within the present conditions. Also encouraging was the banded pattern of RyR3 expression (Figs 1 and 2) indicative that it may have reached the right location to amplify RyR1-mediated voltage-activated Ca^{2+} release and produce spark-like Ca^{2+} release events. Control and RyR3- expressing fibres were injected with fluo-3, voltage-clamped at −80 mV, and depolarizing pulses applied while taking confocal images in line-scan mode (1.54 ms per line). Figure 6*A* shows global fluo-3 Ca^{2+} transients elicited by 500 ms-long depolarizing pulses to −50, −45 and −40 mV in a control fibre (left) and in a RyR3-expressing fibre (right). Traces were obtained by averaging all values at a given time within an (x,t) image like the ones shown in Fig. 6*B–D*. Of course, in the case of the RyR3-positive fibres, the position of the line was set within the expression area. There was no drastic alteration of the overall time course of global change in the fluo-3 signal in the RyR3-expressing fibres: the fluorescence signal rose continuously during the depolarization and started to decay as soon as the membrane was repolarized. The peak $\Delta F/F$ value measured at the end of the depolarizing pulses also appeared not to strongly differ between control and RyR3-expressing fibres. For instance in response to a depolarization to −40 mV it was 2.1 ± 0.13 in control fibres ($n = 5$) and 1.74 ± 0.17 in RyR3-expressing fibres ($n = 7$). However, we wish to be careful when comparing these values because GFP contributed to the baseline fluorescence in the RyR3-expressing fibres so that the amplitude of the transients may have been, to some extent, underestimated (see Methods). Furthermore, a careful comparison of the global voltage-induced Ca^{2+} release

© 2008 The Authors. Journal compilation © 2008 The Physiological Society

between control and RyR3-expressing fibres would require exploring the properties of the signals elicited by larger voltage-clamp depolarizations (0 to +20 mV) for which Ca^{2+} release gets maximally activated. Under the present conditions this, however, inevitably produced large contractile artefacts that precluded analysis of the Ca^{2+} transients.

Figure 6*B* and *C* shows actual (*x*,*t*) images of the fluo-3 fluorescence taken from a control and a RyR3-expressing fibre depolarized by a 500 ms pulse. The time course of the normalized fluorescence change at a given position within the line (marked by an arrow) is shown underneath each image. There was no qualitative difference between the two images; the pulse generated a diffuse elevation of fluorescence devoid of detectable discrete events having the properties of Ca^{2+} sparks, as previously described in rat and mouse muscle fibres (Shirokova *et al.* 1998; Csernoch *et al.* 2006). Conversely, Fig. 6*D* shows an (*x*,*t*) image taken

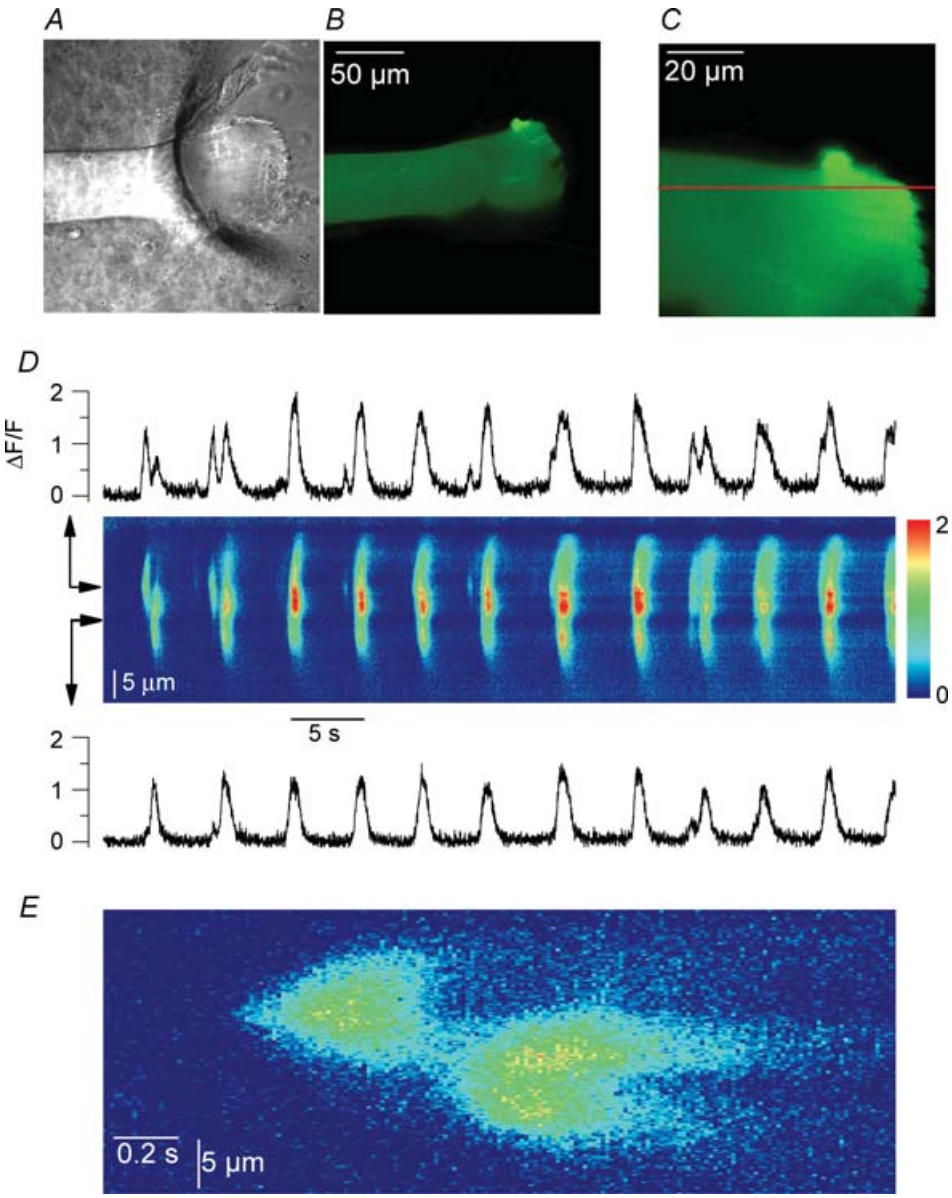

Figure 4. Spontaneous Ca^{2+} release activity detected in line-scan mode from a RyR3-expressing muscle fibre

A and *B*, transmitted light image and corresponding confocal fluorescence image from the silicone-free end area of a RyR3-expressing fibre microinjected with fluo-3. *C*, enlarged confocal view of the RyR3-positive area. The horizontal line shows the position of the line-scan. *D*, (*x*,*t*) image obtained from a portion of the scanned line where repetitive Ca^{2+} release events were detected. The time course of relative change in fluorescence at two distinct locations of the line is shown above and below the image. *E*, enlarged view of the first two events in the image shown in *D*. The fibre was voltage-clamped and held at −80 mV throughout.

© 2008 The Authors. Journal compilation © 2008 The Physiological Society

under the same conditions from a frog fibre. As expected, the image was packed with discrete highly fluorescent events during the pulse, corresponding to Ca^{2+} sparks. We collected a total of 50 (x,t) images from 11 RyR3-expressing fibres under the conditions of Fig. 6 and looked for spark-like discrete local events within the depolarization interval. There were none. We could not find any sign of voltage-activated Ca^{2+} sparks in these RyR3-expressing fibres. In five of these images voltage-evoked Ca^{2+} release and RyR3-related spontaneous Ca^{2+} release activity were simultaneously observed. Figure 7 shows two of those images. In Fig. 7*A* voltage-evoked Ca^{2+} release was coincidently triggered while there was activation of a large long-lasting spontaneous Ca^{2+} transient. In Fig. 7*B*, a more local spontaneous Ca^{2+} oscillation occurred after the end of the depolarization. Under these conditions there is no doubt that functional RyR3 channels were present within the scanned region of the fibre but still, no Ca^{2+} spark was triggered by the depolarization. Interestingly, within such images, the voltage-evoked initial rise in fluo-3 fluorescence appeared to be reduced within the line portion where the spontaneous Ca^{2+} release activity occurred. This is also illustrated by the time courses of change in normalized fluorescence at distinct positions (indicated by arrows) along the line, shown underneath each image. The voltage-evoked initial peak rate of rise in normalized fluo-3 fluorescence was estimated from the first derivative of such time courses. On average this initial peak rate was reduced by $44 \pm 2\%$ $(n = 5)$ within the line region where spontaneous activity occurred as compared to control regions of the line. This indicates that the RyR3-related spontaneous Ca^{2+} release activity interfered with normal voltage-activated Ca^{2+} release.

Voltage-induced rhod-2 Ca^{2+} signals in RyR3-expressing fibres

In order to accurately compare the properties of global voltage-activated Ca^{2+} release in the presence and absence of RyR3, a specific series of experiments was performed using the dye rhod-2 in place of fluo-3. Fibres expressing the GFP-RyR3 construct were injected with rhod-2 and line-scan images (1.54 ms per line) of rhod-2 fluorescence were taken while voltage-clamp depolarizing pulses were applied. All experiments were performed so that, within the silicone-free portion of fibre under voltage clamp,

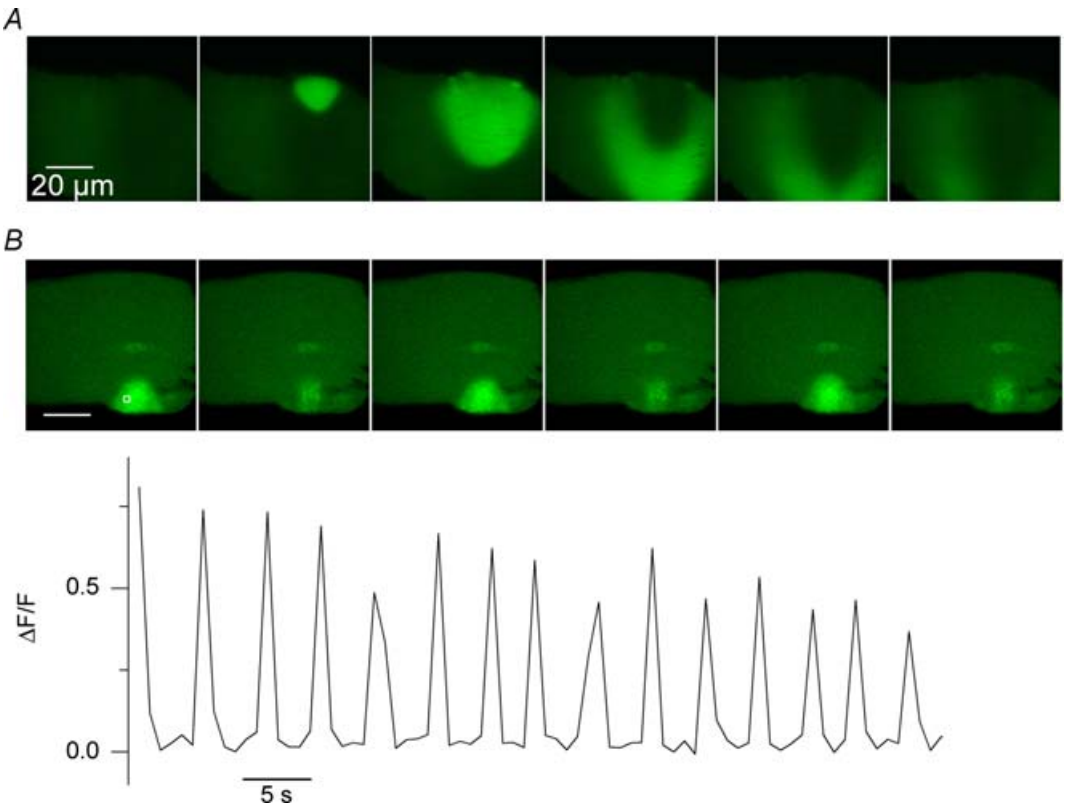

Figure 5. Spontaneous $[Ca^{2+}]$ oscillations in RyR3-expressing muscle fibres sometimes propagate (*A*) and persist in the absence of extracellular calcium (*B*)
Both panels show a sequence of consecutive confocal fluorescence images from a RyR3-expressing region of fibre. In *A* and *B*, images shown were taken every 0.8 and 2.4 s, respectively. In *B*, the graph shows the time course of relative change in fluorescence within the area highlighted by a white box in the first image.

© 2008 The Authors. Journal compilation © 2008 The Physiological Society

the scanned line included on one side a region where GFP-RyR3 expression was maximal and, on the other side, a region where the expression was the lowest possible, which we will refer to as the corresponding control region of fibre. In this way we could specifically compare voltage-activated Ca^{2+} release measured simultaneously within a clearly identified RyR3-positive region and within a control region of the same fibre portion where expression was much less. Measurements were restricted to fibres that yielded no clear spontaneous

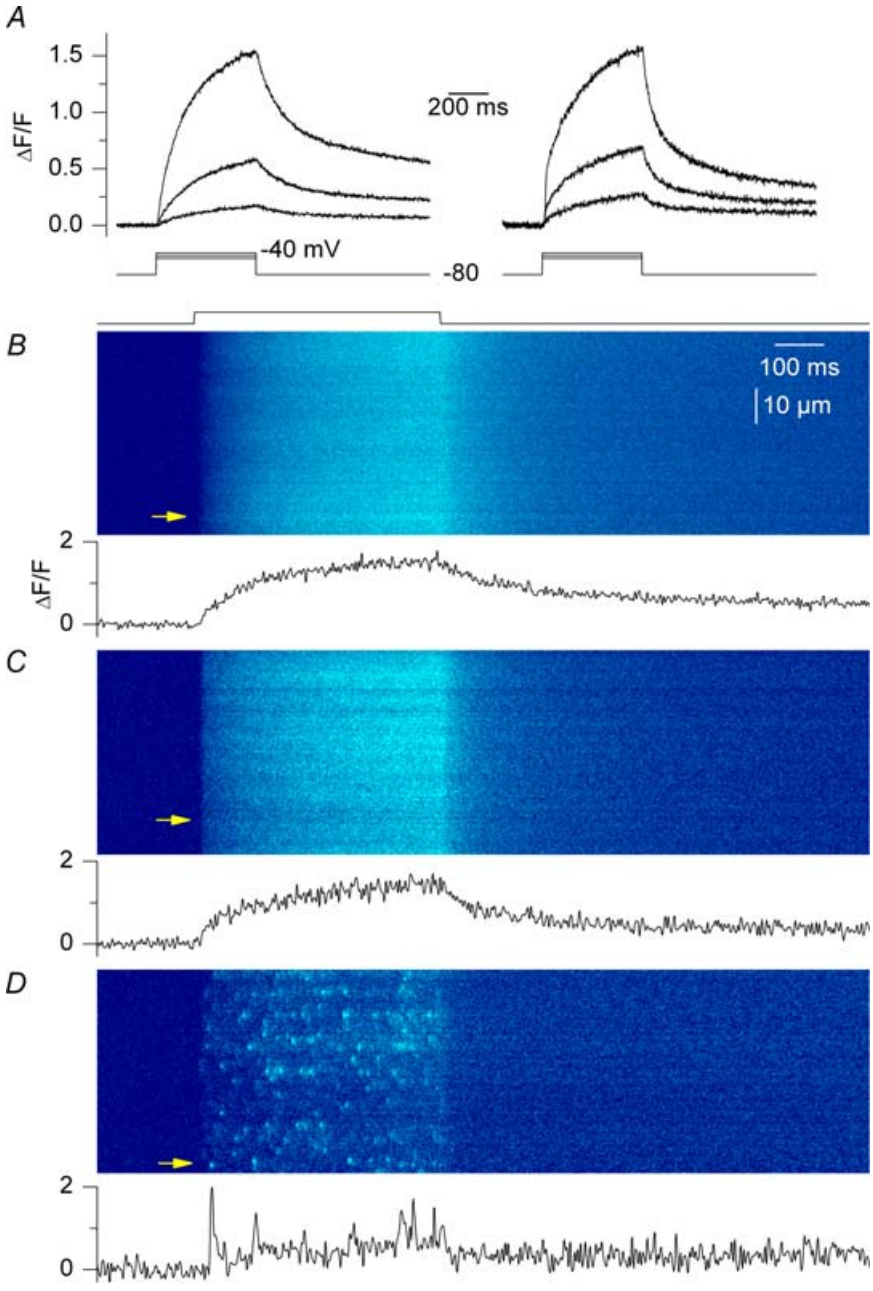

Figure 6. Voltage-induced Ca^{2+} signals in line-scan mode
Confocal (*x,t*) line-scan images were taken from fluo-3-injected control fibres, RyR3-positive fibres and frog fibres that were depolarized by voltage-clamp pulses. *A*, global fluo-3 Ca^{2+} transients elicited by 500 ms-long depolarizing pulses to −50, −45 and −40 mV in a control fibre (left) and in the positive region of a RyR3-expressing fibre (right); transients were obtained by averaging all lines in a given (*x,t*) image. *B–D*, *(x,t)* images taken from a control fibre, a RyR3-expressing fibre and a frog fibre that were depolarized by a 500 ms-long pulse to −40, −40 and −50 mV, respectively. The trace below each image shows the time course of change in fluorescence at the position indicated by the arrow.

© 2008 The Authors. Journal compilation © 2008 The Physiological Society

Ca^{2+} release activity to limit possible interferences with voltage-activated Ca^{2+} release. We managed to take such records in six GFP-RyR3-positive fibres. Figure 8 illustrates the results from these measurements. Figure 8*A* shows an illustrative example of a pair of confocal images taken from a given portion of a GFP-RyR3-positive fibre; the left panel shows the GFP-RyR3 fluorescence that yielded the typical local banded pattern whereas the right panel shows the corresponding rhod-2 fluorescence that was distributed throughout the entire fibre volume. Figure 8*B* shows an (x,t) confocal line-scan image of the normalized rhod-2 fluorescence taken from a portion of fibre that included a GFP-RyR3-positive region; (x,y) images of the GFP-RyR3 fluorescence and of the rhod-2 fluorescence from the corresponding fibre portion are shown at the top of Fig. 8*B*, with the position of the scanned line indicated in yellow. The fibre was depolarized by a 500 ms-long pulse to −35 mV. In Fig. 8*B*, the graph on the left of the (x,t) image corresponds to the profile of the GFP-RyR3 fluorescence along the scanned line; RyR3 expression was maximal in the top region of the image (*b*) as compared to the bottom region (*a*). Forty-two such images were collected from the six studied fibres and again, under these conditions, no Ca^{2+} spark could ever be triggered by a voltage pulse within the RyR3-positive region of the fibres. Figure 8*C* shows the time course of normalized change in rhod-2 fluorescence within the GFP-RyR3-positive region of the line (*b*, red trace) and within the control region of the line (*a*, black trace). The time course was calculated from the average of 50 adjacent rows within each of the two regions of interest (*a* and *b*). Results illustrate the fact that the peak amplitude of the voltage-activated Ca^{2+} transient was not strongly altered in a reproducible manner within the GFP-RyR3-expressing region as compared to the

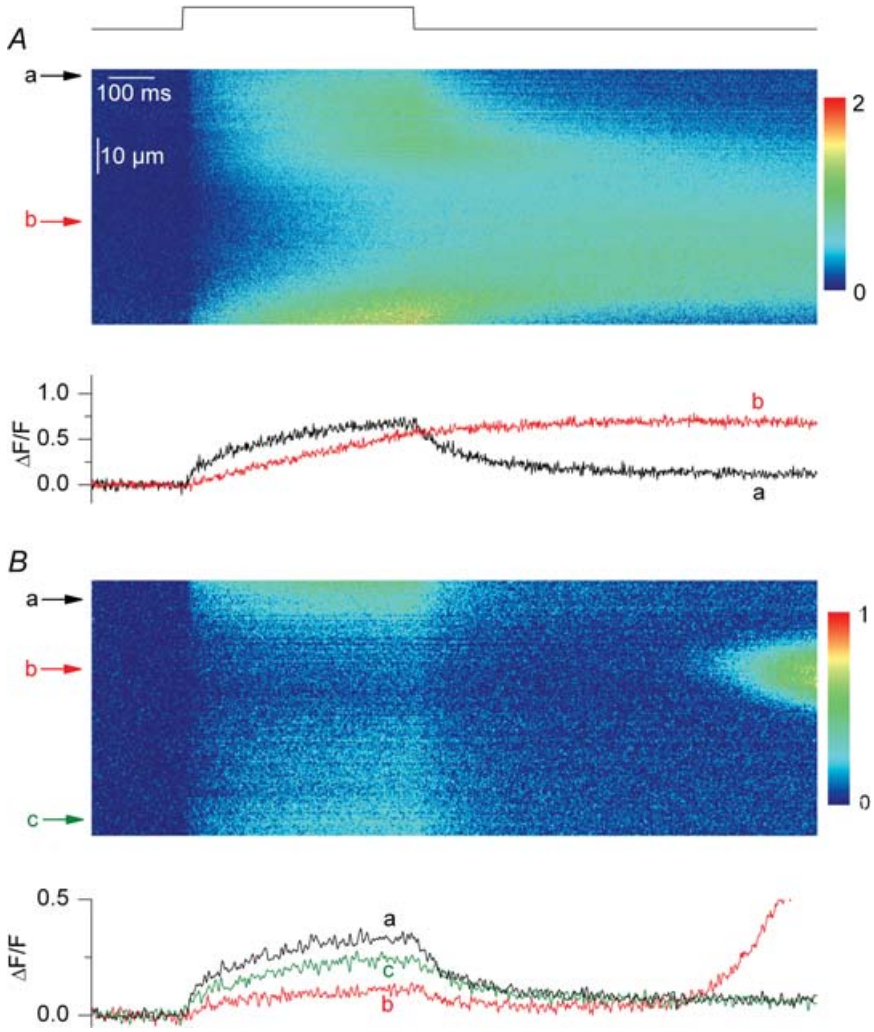

Figure 7. Line-scan images from RyR3-expressing muscle fibres exhibiting voltage-induced Ca^{2+} signals and spontaneous Ca^{2+} release activity
The traces below each image show the time course of change in fluorescence at the positions indicated by the corresponding arrows in the line-scan image. Time courses are from the average of three neighbouring lines.

© 2008 The Authors. Journal compilation © 2008 The Physiological Society

control region of a same fibre. An analysis was carried out on such pairs of signals evoked by pulses to values ranging between −40 and −30 mV; results from the several images taken in each fibre were pooled and averaged. The mean ratio of the amplitude of the rhod-2 $\Delta F/F$ fluorescence signal (measured at the time of the end of the pulse) within the RyR3-positive regions to the one measured within the corresponding control regions was 1.36 ± 0.25 ($n = 6$), not significantly different from unity ($P = 0.2$, $n = 6$). However, it can be seen in Fig. 8*C* that the rhod-2 fluorescence trace from the RyR3-expressing region exhibited a larger initial peak phase than the trace from the corresponding control region, suggesting a larger initial rate of Ca^{2+} release. In order to quantitatively investigate this feature we estimated the Ca^{2+} release flux from the rhod-2 fluorescence transients. Figure 8*D* shows the Ca^{2+} release flux traces calculated from the above corresponding rhod-2 signals, as described in Methods. The flux measured in the RyR3-expressing region exhibited a definitely prominent early peak as compared to the flux from the corresponding control region. Conversely, the flux at the time of the end of the pulse was very similar in the two regions. This came out to be a reproducible difference between the RyR3-positive regions and the control regions of the fibres. The mean ratio of the initial peak flux value measured within the RyR3-expressing region of fibres to the corresponding initial flux value in the control region was 1.3 ± 0.09 ($n = 6$), significantly different from unity. In contrast, the mean ratio of the end-pulse flux in the RyR3-expressing regions to the end-pulse flux in the corresponding control regions did not significantly differ from unity (1.1 ± 0.08). We also calculated values for the ratio of the peak to the end-pulse flux in the control and in the RyR3-expressing regions of the fibres. As illustrated in Fig. 8*E* the mean value for this ratio in the RyR3-expressing regions was 1.3 ± 0.05, significantly larger than the mean value in the control regions (1.0 ± 0.02, $P = 0.03$). The results clearly demonstrate that the expression of RyR3 was associated with the presence of a prominent initial phase during the time course of the release flux.

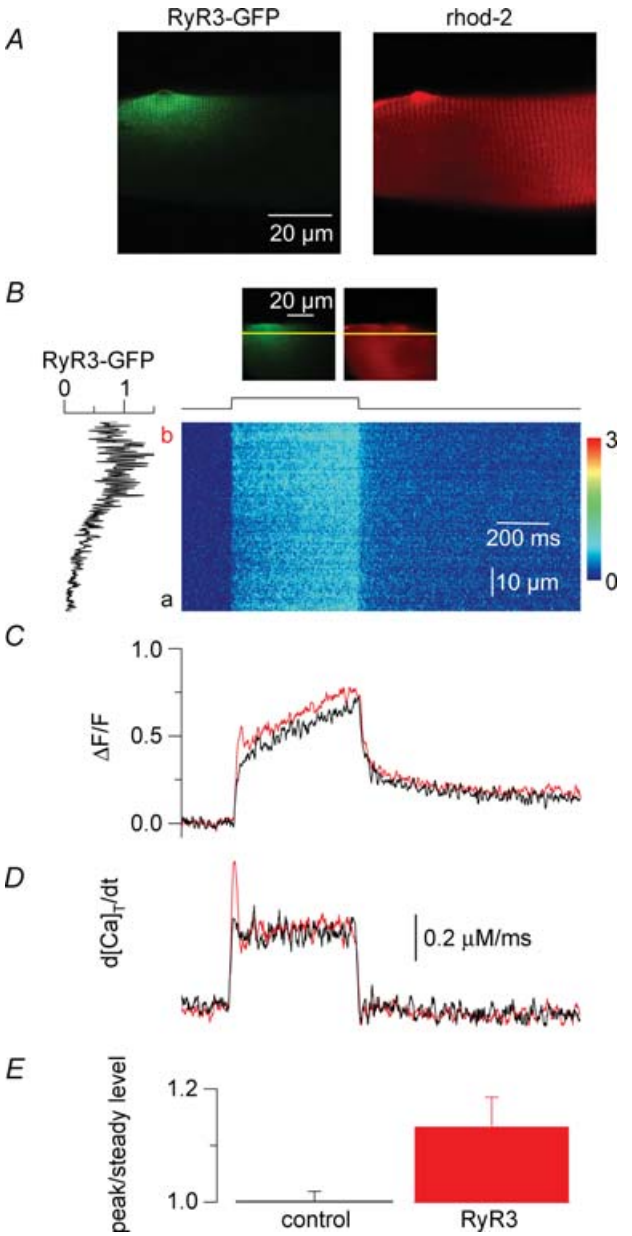

Figure 8. Voltage-activated Ca^{2+} release flux measured with rhod-2 in control and RyR3-expressing regions of the same muscle fibres
A, confocal (*x,y*) images of the GFP-RyR3 fluorescence (left) and of the rhod-2 fluorescence from a same portion of muscle fibre (right). *B*, confocal (*x,t*) line-scan image of the rhod-2 fluorescence taken from a region of fibre that included a GFP-RyR3-positive area; the fibre was depolarized by a 500 ms-long pulse from −80 mV to −35 mV. The graph on the left shows the profile of the GFP-RyR3 fluorescence along the line. The two frames on top correspond to (*x,y*) images of the GFP-RyR3 fluorescence and of the rhod-2 fluorescence from the corresponding fibre portion with the position of the scanned line indicated in yellow. *C*, time course of change in normalized rhod-2 fluorescence elicited by the pulse within the regions *a* (black trace, control) and *b* (red trace, RyR3 positive) of the line. *D*, Ca^{2+} release flux traces calculated from the above corresponding rhod-2 transients. *E*, mean values for the ratio of the initial peak Ca^{2+} release flux (peak) to its value at the end of the pulse (steady level) in the control and GFP-RyR3-expressing regions of fibres.

Expression of a GFP-RyR1 construct

In order to check whether the effects reported here were specific to the RyR3 isoform and would not result simply from over-expression of any RyR channel, we transfected muscle fibres with a GFP-RyR1 construct. There was no gross difference in terms of transfection efficiency and pattern of expression between the GFP-RyR3 and GFP-RyR1 constructs. With RyR1, the number of positive fibres per muscle was also small and the fluorescence was distributed within one or a few local areas of the fibres. Figure 9*A* shows a confocal fluorescence image (right) and the corresponding transmitted light image (left) taken

© 2008 The Authors. Journal compilation © 2008 The Physiological Society

from a muscle fibre expressing the RyR1 construct. The average profile of the fluorescence intensity from the region highlighted by a white box is shown below. As in the case of RyR3, the fluorescence exhibited a sarcomere-related banded pattern with a periodicity of about 1 μm. Figure 9*B* shows a confocal image of the same field taken after fluo-3 had been injected and diffused throughout the fibre. Figure 9*C* shows a series of consecutive confocal frames taken from that fibre at 1.25 Hz. There was no sign whatsoever of spontaneous Ca^{2+} release activity. Figure 9*D* shows an (x,t) line-scan image taken from the GFP-positive area of another RyR1-transfected fibre, also illustrating the absence of Ca^{2+} release activity. The same result was obtained in 16 other GFP-RyR1-positive fibres that were injected with fluo-3. This shows that the spontaneous Ca^{2+} release activity observed in the presence of RyR3 cannot simply be reproduced by the over-expression of any RyR isoform.

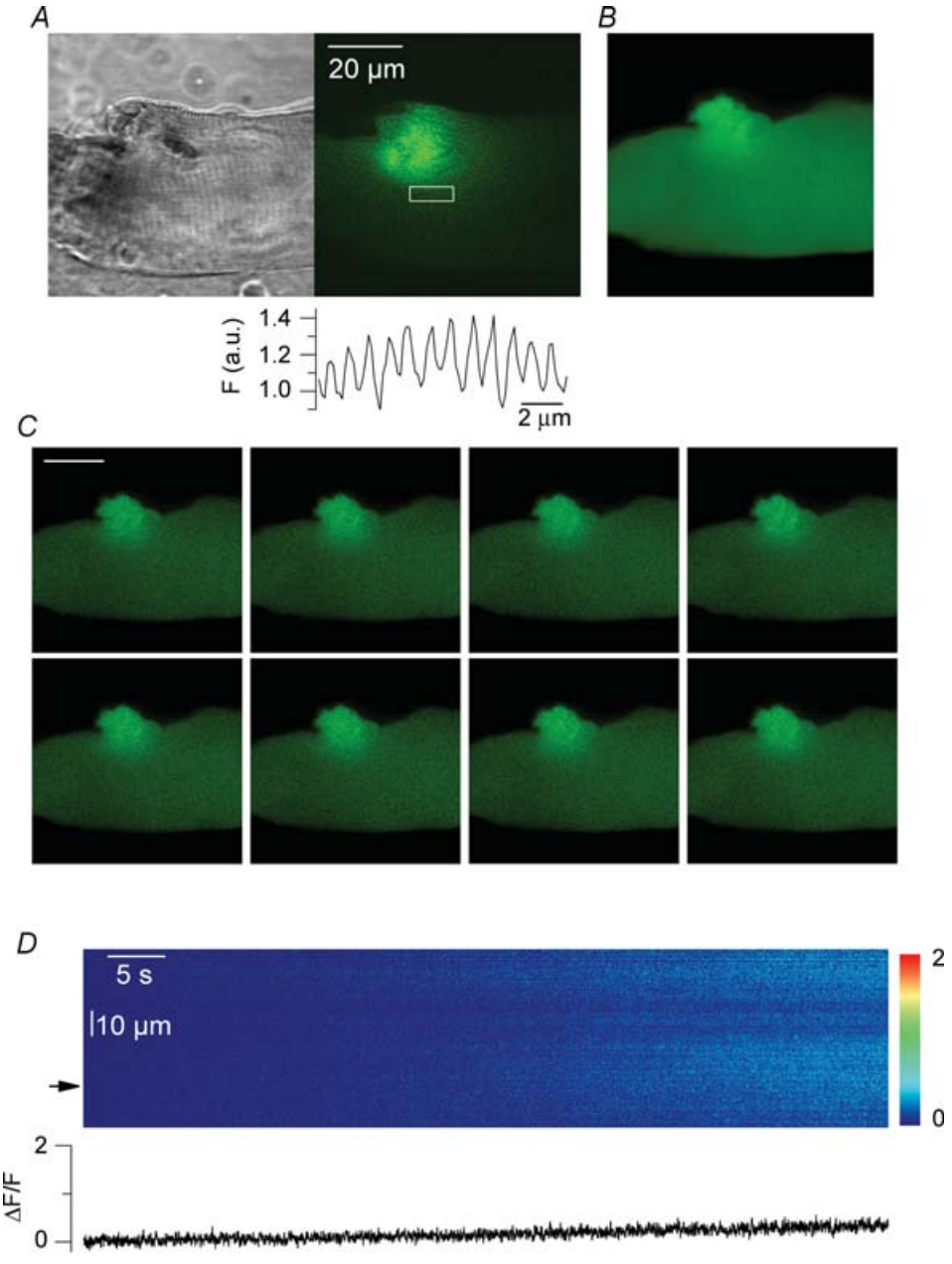

Figure 9. Expression of GFP-tagged RyR1 channels in mouse skeletal muscle fibres
A, confocal fluorescence image (right) and corresponding transmitted light image (left) taken from a muscle fibre expressing the GFP-RyR1 DNA construct. The average profile of the fluorescence intensity from the region highlighted by a white box is shown below. *B*, confocal image of the same field taken after fluo-3 had been injected and diffused throughout the fibre. *C*, series of consecutive confocal frames taken from that fibre at 1.25 Hz. *D*, (x,t) line-scan image taken from the GFP-positive area of another GFP-RyR1-positive region of fibre.

© 2008 The Authors. Journal compilation © 2008 The Physiological Society

Discussion

We demonstrate here that RyR3 channels expressed in adult mouse skeletal muscle fibres are capable of sustaining a robust Ca^{2+} release activity that operates independently from the normal voltage-dependent control of the endogenous RyR channels. The use of a GFP-RyR3 construct allowed us to unambiguously identify the transfected muscle fibres that could then be selected for intracellular Ca^{2+} measurements. It also enabled an accurate characterization of the RyR3 expression pattern of the studied cells: under our conditions, RyR3 was expressed within restricted areas of the fibres, most usually in the vicinity of one nucleus. The reason for this non-homogeneous expression is unclear. It may be that either access of the plasmid was somehow only granted to a restricted number of nuclei and that the synthesized RyR3s did not reach regions of the fibres distant from those or that the nuclei population was not homogeneous in terms of transcriptional activity. Another important feature of the transfected fibres was that the subcellular GFP-RyR3 fluorescence pattern was consistent with RyR3 being within the junctional SR membrane, a strategic position in regard to the possibility of this channel contributing to voltage-activated SR Ca^{2+} release. This specific location was confirmed by immunostaining which also revealed that RyR1 channels were still present together with RyR3 within the expression areas, although we could not precisely assess the relative amount of the two isoforms. Overall, despite the quite low transfection efficiency, this experimental model appeared well suited to characterize the functional properties of RyR3 *in vivo*. The most obvious consequence of the presence of RyR3 on intracellular Ca^{2+} homeostasis was an almost systematic oscillating Ca^{2+} release activity within the region of expression. This very spectacular spontaneous phenomenon never occurs in an intact skeletal muscle fibre where, under normal conditions, SR Ca^{2+} release always remains tightly controlled by the plasma membrane polarization. Instead, the RyR3 expression-induced spontaneous activity was maintained in cells voltage-clamped at resting potential levels and could still be detected in the absence of extracellular calcium, indicating that it was not triggered by an electrical activity and/or a transmembrane Ca^{2+} influx. Also interesting is that the RyR3-related spontaneous Ca^{2+} transients were in some cases large enough to drive local contractions, witnessing a very substantial amount of Ca^{2+} released from the SR under these conditions. Although we cannot exclude the possibility that RyR1 channels either contributed to or were necessary for this spontaneous activity, we believe that it is more likely to solely result from properties inherent in the RyR3 isoform because it did not occur when the GFP-RyR1 channel was expressed. This isoform specificity in terms of cellular Ca^{2+} signals is also consistent with results from the expression of RyR1 and RyR3 in a heterologous cell system (Rossi *et al.* 2002). The spatio-temporal features of the spontaneous Ca^{2+} release activity recorded here were highly variable from fibre to fibre but always appeared to largely exceed those of the most conventional Ca^{2+} release events, the 'Ca^{2+} sparks', that can be detected under particular conditions of stress in this same preparation (Kirsch *et al.* 2001; Wang *et al.* 2005). This suggests that the coherent or propagative recruitment of large arrays of RyR3 channels was responsible for the spontaneous Ca^{2+} release activity that we observed. Further in-depth studies of this particular phenomenon should help us uncover the mechanisms that lead to the activation and closure of the RyR3 channels *in vivo* and provide insights into their potential role within cell types where they are endogenously expressed.

Now, having functional RyR3 channels, coexpressed with RyR1 channels, within the triadic environment of an adult mammalian muscle fibre appeared to be a very promising situation to reveal the role of these channels in the production of voltage-activated Ca^{2+} sparks. Indeed this situation approaches the frog muscle model, which contains two RyR isoforms respectively homologous to RyR1 and RyR3 (Lai *et al.* 1992), and which produces Ca^{2+} sparks in response to membrane depolarization (Tsugorka *et al.* 1995; Klein *et al.* 1996). However, in our hands, the combination of voltage-clamp depolarization with confocal line-scan measurements of fluo-3 fluorescence failed to reveal the presence of resolvable specific discrete Ca^{2+} release events in the RyR3-expressing fibres. Instead the confocal images only exhibited a diffuse increase in fluo-3 fluorescence in response to the pulse, as previously described in normal mammalian muscle fibres (Shirokova *et al.* 1998). This was also true when line-scan images included both spontaneous RyR3-related Ca^{2+} release macro-events and voltage-activated Ca^{2+} release (Fig. 7), a condition under which the presence of functional RyR3 channels in the confocal plane was hardly deniable. The fact that, under these conditions, voltage-activated Ca^{2+} release appeared to be depressed within the regions of spontaneous Ca^{2+} release activity may be speculated to result from this activity producing local SR Ca^{2+} depletion. At last, the lack of voltage-activated Ca^{2+} sparks in the RyR3-expressing regions of fibres was also confirmed in a series of experiments performed with the dye rhod-2 which allowed us to measure Ca^{2+} changes within unambiguously identified RyR3-positive regions of fibres. It may be argued that the GFP tag somehow either prevented correct targeting of the RyR3 channels within the triadic environment or that it influenced the functional behaviour of the channel so as to prevent the production of Ca^{2+} sparks. However, analysis of the global voltage-activated Ca^{2+} transients revealed the presence of a prominent early component of the Ca^{2+}

© 2008 The Authors. Journal compilation © 2008 The Physiological Society

release flux within RyR3-positive regions of fibres as compared to control regions. This strongly supports the possibility that the GFP-RyR3 channels contributed to voltage-activated Ca^{2+} release and thus, that the GFP tag did not prevent their adequate localization and proper function within the normal EC coupling process. In frog muscle, the presence of such an early peak has, for a long time, been postulated to result from Ca^{2+}-induced Ca^{2+} release (see for instance Jacquemond *et al.* 1991). Present results would agree with the possibility that, under our conditions, GFP-RyR3 channels were capable of contributing to the voltage-activated Ca^{2+} release flux through a similar process. Still, in terms of elementary Ca^{2+} release the simplest conclusion from our measurements is that supplementing mammalian muscle fibres with functional RyR3 channels is not sufficient for producing voltage-activated Ca^{2+} sparks.

Interestingly, Pouvreau *et al.* (2007) recently came to an opposite conclusion using an overall experimental approach similar to the one used here; under their conditions, certain fibres isolated from RyR3-transfected mouse muscles produced a spontaneous Ca^{2+} release activity that appeared to yield qualitative properties more or less similar to what we describe here. According to their results, regions of fibres yielding this activity were also endowed with Ca^{2+} sparks triggered by voltage-clamp depolarization. The absence of such events under our conditions is puzzling and there are quite a number of specific differences between the two studies that may be speculated to be involved. Among these, technical differences in the transfection procedures may play a role, leading to fibres that one may suspect to either express a qualitatively/quantitatively different pattern/level of RyR3 channels or to yield other differences in terms of functional properties. More specifically, Pouvreau *et al.* (2007) used hyaluronidase before plasmid injection, subcutaneous electrodes for the electroporation process and studied fibres isolated 6–10 days after transfection. Conversely, we used somewhat more gentle conditions of transfection: we did not use hyaluronidase, performed electroporation with extra-cutaneous electrodes and waited 2 weeks before isolating fibres from the transfected muscles. There are also specific differences in the experimental conditions between the two studies that may be important. In our case, we microinjected the Ca^{2+} dye and performed measurements on a restricted portion of fibre reliably maintained under voltage clamp through the silicone-insulation process, and this, under non-intracellular Ca^{2+}-buffering conditions. As illustrated in Fig. 6, these conditions, when applied to frog muscle fibres, proved to effortlessly produce unmistakable Ca^{2+} sparks upon membrane depolarization, whereas we were unable to trigger one such event within any of the well-identified RyR3-positive portions of fibres under voltage clamp. On the other hand, Pouvreau *et al.* (2007) used AM loading of the Ca^{2+} dye and applied the whole-cell patch-clamp technique to the entire fibres using a pipette containing 1–5 mM EGTA and they assessed the presence of a RyR3-positive region of fibre from the occurrence of spontaneous Ca^{2+} release activity. Again, one or a combination of several of these experimental discrepancies may also be speculated to influence the capacity of fibres to produce voltage-activated Ca^{2+} sparks. Future studies aimed at understanding the reason for the different results will certainly provide interesting clues concerning the mechanisms involved in the generation of voltage-activated Ca^{2+} sparks. At present, our data show that the combined presence of RyR1 and RyR3 in a mammalian muscle fibre is not enough *per se* for membrane depolarization to trigger such Ca^{2+} release events.

On top of this stimulating controversy, the present results demonstrate that in this highly differentiated cell type, the RyR3 Ca^{2+} release channels exhibit an intrinsic propensity to generate voltage-free cytoplasmic Ca^{2+} oscillations. We believe that this is not an artefact from over-expression of the channel because it was not reproduced when RyR1 was expressed under the same conditions. It is then interesting to speculate that, *in vivo*, the transient or chronic expression of this particular Ca^{2+} release channel may be physiologically intended to serve specific Ca^{2+}-dependent signalling pathways independent from changes in plasma membrane ion channel- and/or electrical-activity.

References

Baylor SM (2005). Calcium sparks in skeletal muscle fibers. *Cell Calcium* **37**, 513–530.

Bertocchini F, Ovitt CE, Conti A, Barone V, Scholer HR, Bottinelli R, Reggiani C & Sorrentino V (1997). Requirement for the ryanodine receptor type 3 for efficient contraction in neonatal skeletal muscles. *EMBO J* **16**, 6956–6963.

Bruce JI, Straub SV & Yule DI (2003). Crosstalk between cAMP and Ca^{2+} signaling in non-excitable cells. *Cell Calcium* **34**, 431–444.

Cheng H, Lederer WJ & Cannell MB (1993). Calcium sparks: elementary events underlying excitation-contraction coupling in heart muscle. *Science* **262**, 740–744.

Collet C, Pouvreau S, Csernoch L, Allard B & Jacquemond V (2004). Calcium signaling in isolated skeletal muscle fibers investigated under 'Silicone Voltage-Clamp' conditions. *Cell Biochem Biophys* **40**, 225–236.

Conklin MW, Barone V, Sorrentino V & Coronado R (1999). Contribution of ryanodine receptor type 3 to Ca^{2+} sparks in embryonic mouse skeletal muscle. *Biophys J* **77**, 1394–1403.

Conti A, Reggiani C & Sorrentino V (2005). Selective expression of the type 3 isoform of ryanodine receptor Ca^{2+} release channel (RyR3) in a subset of slow fibers in diaphragm and cephalic muscles of adult rabbits. *Biochem Biophys Res Commun* **337**, 195–200.

© 2008 The Authors. Journal compilation © 2008 The Physiological Society

Csernoch L, Bernengo JC, Szentesi P & Jacquemond V (1998). Measurements of intracellular Mg^{2+} concentration in mouse skeletal muscle fibers with the fluorescent indicator mag-indo-1. *Biophys J* **75**, 957–967.

Csernoch L, Pouvreau S & Jacquemond V (2006). Voltage-activated calcium release events in mouse skeletal muscle fibers. *Biophys J* **90**, B192.

Dietze B, Bertocchini F, Barone V, Struk A, Sorrentino V & Melzer W (1998). Voltage-controlled Ca^{2+} release in normal and ryanodine receptor type 3 (RyR3)-deficient mouse myotubes. *J Physiol* **513**, 3–9.

Felder E & Franzini-Armstrong C (2002). Type 3 ryanodine receptors of skeletal muscle are segregated in a parajunctional position. *Proc Natl Acad Sci U S A* **99**, 1695–1700.

Fessenden JD, Wang Y, Moore RA, Chen SR, Allen PD & Pessah IN (2000). Divergent functional properties of ryanodine receptor types 1 and 3 expressed in a myogenic cell line. *Biophys J* **79**, 2509–2525.

Fill M & Copello JA (2002). Ryanodine receptor calcium release channels. *Physiol Rev* **82**, 893–922.

Flucher BE, Conti A, Takeshima H & Sorrentino V (1999). Type 3 and type 1 ryanodine receptors are localized in triads of the same mammalian skeletal muscle fibers. *J Cell Biol* **146**, 621–630.

Giannini G, Clementi E, Ceci R, Marziali G & Sorrentino V (1992). Expression of a ryanodine receptor-Ca^{2+} channel that is regulated by TGF-β. *Science* **257**, 91–94.

Jacquemond V (1997). Indo-1 fluorescence signals elicited by membrane depolarization in enzymatically isolated mouse skeletal muscle fibers. *Biophys J* **73**, 920–928.

Jacquemond V, Csernoch L, Klein MG & Schneider MF (1991). Voltage-gated and calcium-gated calcium release during depolarization of skeletal muscle fibers. *Biophys J* **60**, 867–873.

Kirsch WG, Uttenweiler D & Fink RH (2001). Spark- and ember-like elementary Ca^{2+} release events in skinned fibres of adult mammalian skeletal muscle. *J Physiol* **537**, 379–389.

Klein MG, Cheng H, Santana LF, Jiang YH, Lederer WJ & Schneider MF (1996). Two mechanisms of quantized calcium release in skeletal muscle. *Nature* **379**, 455–458.

Lai FA, Liu QY, Xu L, el-Hashem A, Kramarcy NR, Sealock R & Meissner G (1992). Amphibian ryanodine receptor isoforms are related to those of mammalian skeletal or cardiac muscle. *Am J Physiol Cell Physiol* **263**, C365–C372.

Legrand C, Giacomello E, Berthier C, Allard B, Sorrentino V & Jacquemond V (2007). Ca^{2+} signals in adult mouse skeletal muscle fibers expressing type 3 ryanodine receptor (RyR3). 2007 Biophysical Society Meeting Abstracts. *Biophys J* (Suppl.), 312a, Abstract, 1470-Pos.

Nakai J, Ogura T, Protasi F, Franzini-Armstrong C, Allen PD & Beam KG (1997). Functional nonequality of the cardiac and skeletal ryanodine receptors. *Proc Natl Acad Sci U S A* **97**, 157–162.

Ottini L, Marziali G, Conti A, Charlesworth A & Sorrentino V (1996). α and β isoforms of ryanodine receptor from chicken skeletal muscle are the homologues of mammalian RyR1 and RyR3. *Biochem J* **315**, 207–216.

Oyamada H, Murayama T, Takagi T, Iino M, Iwabe N, Miyata T, Ogawa Y & Endo M (1994). Primary structure and distribution of ryanodine-binding protein isoforms of the bullfrog skeletal muscle. *J Biol Chem* **269**, 17206–17214.

Pouvreau S, Csernoch L, Allard B, Sabatier JM, De Waard M, Ronjat M & Jacquemond V (2006). Transient loss of voltage control of Ca^{2+} release in the presence of maurocalcine in skeletal muscle. *Biophys J* **91**, 2206–2215.

Pouvreau S, Royer L, Yi J, Brum G, Meissner G, Rios E & Zhou J (2007). Ca^{2+} sparks operated by membrane depolarization require isoform 3 ryanodine receptor channels in skeletal muscle. *Proc Natl Acad Sci U S A* **104**, 5235–5340.

Rossi D, Simeoni I, Micheli M, Bootman M, Lipp P, Allen PD & Sorrentino V (2002). RyR1 and RyR3 isoforms provide distinct intracellular Ca^{2+} signals in HEK 293 cells. *J Cell Sci* **115**, 2497–2504.

Rossi D & Sorrentino V (2002). Molecular genetics of ryanodine receptors Ca^{2+}-release channels. *Cell Calcium* **32**, 307–319.

Shirokova N, Garcia J & Rios E (1998). Local calcium release in mammalian skeletal muscle. *J Physiol* **512**, 377–384.

Shirokova N, Shirokov R, Rossi D, Gonzalez A, Kirsch WG, Garcia J, Sorrentino V & Rios E (1999). Spatially segregated control of Ca^{2+} release in developing skeletal muscle of mice. *J Physiol* **521**, 483–495.

Sorrentino V (2003). Ryanodine receptor type 3: why another ryanodine receptor isoform? *Front Biosci* **8**, 176–182.

Tarroni P, Rossi D, Conti A & Sorrentino V (1997). Expression of the ryanodine receptor type 3 calcium release channel during development and differentiation of mammalian skeletal muscle cells. *J Biol Chem* **272**, 19808–19813.

Tsugorka A, Rios E & Blatter LA (1995). Imaging elementary events of calcium release in skeletal muscle cells. *Science* **269**, 1723–1726.

Wang X, Weisleder N, Collet C, Zhou J, Chu Y, Hirata Y, Zhao X, Pan Z, Brotto M, Cheng H & Ma J (2005). Uncontrolled calcium sparks act as a dystrophic signal for mammalian skeletal muscle. *Nat Cell Biol* **7**, 525–530.

Ward CW, Protasi F, Castillo D, Wang Y, Chen SR, Pessah IN, Allen PD & Schneider MF (2001). Type 1 and type 3 ryanodine receptors generate different Ca^{2+} release event activity in both intact and permeabilized myotubes. *Biophys J* **81**, 3216–3230.

Ward CW, Schneider MF, Castillo D, Protasi F, Wang Y, Chen SR & Allen PD (2000). Expression of ryanodine receptor RyR3 produces Ca^{2+} sparks in dyspedic myotubes. *J Physiol* **525**, 91–103.

Yang D, Pan Z, Takeshima H, Wu C, Nagaraj RY, Ma J & Cheng H (2001). RyR3 amplifies RyR1-mediated Ca^{2+}-induced Ca^{2+} release in neonatal mammalian skeletal muscle. *J Biol Chem* **276**, 40210–40214.

Acknowledgements

This work was supported by grants from CNRS, University Claude Bernard Lyon 1 and Association Française contre les Myopathies and grants from Agenzia Spaziale Italiana (ASI) to V. Sorrentino.

Supplemental material

Online supplemental material for this paper can be accessed at:
http://jp.physoc.org/cgi/content/full/jphysiol.2007.145862/DC1
and
http://www.blackwell-synergy.com/doi/suppl/10.1113/jphysiol.2007.145862

© 2008 The Authors. Journal compilation © 2008 The Physiological Society